DATA DRIVEN MODEL BASED LEAST SQUARES IMAGE RECONSTRUCTION FOR RADIO ASTRONOMY

Stefan J. Wijnholds

ASTRON
R & D Department
Oude Hoogeveensedijk 4
NL-7991 PD Dwingeloo
The Netherlands

Alle-Jan van der Veen

Delft University of Technology
Department of Electrical Engineering
Mekelweg 4
NL-2628 CD Delft
The Netherlands

ABSTRACT

Image reconstruction problems in radio astronomy and other fields like biomedical imaging are often ill-posed and some form of regularization is required. This imposes user specified constraints to the reconstruction process that may produce an undesirable bias to the solution. We propose a data driven model based least squares reconstruction method based on the Karhunen-Loève transform. We show that this constraint stems from intrinsic physical properties of the measurement process and demonstrate the improvement of the method over unregularized least squares reconstruction using actual data from the Low Frequency Array (LOFAR), a phased array radio telescope in the Netherlands.

Index Terms— image reconstruction, Karhunen-Loève transform, inversion, regularization, radio astronomy

1. INTRODUCTION

Radio astronomical image reconstruction can be considered a parameter estimation problem in which the pixel values are the parameters to be estimated. This leads to a standard inversion problem for which an l_1- or a least squares (LS) optimized solution can be found [1]. Very similar reconstruction problems are found in other fields like biomedical imaging [2], geophysics [3] and SAR imaging [4]. If the specified image resolution is chosen too high, the problem becomes ill-posed [5, 6] and some form of regularization is required. Regularization imposes user specified constraints to the reconstruction process that may produce an undesirable bias to the solution. After introducing the reconstruction problem in Sec. 2, we therefore propose a data driven model based least squares image reconstruction method based on the Karhunen-Loève transform (KLT) in Sec. 3. We show that this only imposes a constraint that is related to intrinsic physical properties of the instrument. We demonstrate the improvement of our approach over unregularized LS image reconstruction using actual data from the Low Frequency Array (LOFAR) [7], a phased array radio telescope in the Netherlands, in Sec. 4.

This research is being funded by the Dutch government in the BSIK program for interdisciplinary research for improvement of the knowledge infrastructure.

2. PROBLEM STATEMENT

Radio astronomical arrays (and many other sensor arrays) measure the correlations between the output signals of the P receiving elements in the system. This produces a $P \times P$ array covariance matrix that can be modeled as [8]

$$\mathbf{R} = \mathbf{A}\mathbf{\Sigma}\mathbf{A}^H + \mathbf{\Sigma}_{\mathrm{n}}. \quad (1)$$

Here, $\mathbf{\Sigma} = \mathrm{diag}\,(\boldsymbol{\sigma})$ contains the power received from Q directions of arrival, $\mathbf{A}$ describes the array response to the received signals including effects such as propagation phenomena and receiver gain differences, and $\mathbf{\Sigma}_{\mathrm{n}}$ is the noise covariance matrix. We will assume that the latter can be parameterized by a real valued parameter vector $\boldsymbol{\sigma}_{\mathrm{n}}$ that is related to the noise covariance matrix by $\mathrm{vec}\,(\mathbf{\Sigma}_{\mathrm{n}}) = \mathbf{M}_{\mathrm{n}}\boldsymbol{\sigma}_{\mathrm{n}}$. If the image is sampled on a grid, the image vector $\boldsymbol{\sigma}$ represents the power in each of the Q pixels in the image. The image reconstruction problem can be formulated as an estimation problem to find the Q pixel values.

The weighted LS image reconstruction problem can be formulated as

$$\{\widehat{\boldsymbol{\sigma}}, \widehat{\boldsymbol{\sigma}}_{\mathrm{n}}\} = \underset{\boldsymbol{\sigma},\boldsymbol{\sigma}_{\mathrm{n}}}{\mathrm{argmin}} \left\|\mathbf{W}\left(\widehat{\mathbf{r}} - \mathbf{M}\boldsymbol{\sigma} - \mathbf{M}_{\mathrm{n}}\boldsymbol{\sigma}_{\mathrm{n}}\right)\right\|_{\mathrm{F}}^2, \quad (2)$$

where $\|\cdot\|_F$ denotes the Frobenius norm, $\mathbf{W}$ is a weighting matrix, $\widehat{\mathbf{r}} = \mathrm{vec}\left(\widehat{\mathbf{R}}\right)$ is the vectorized version of the array covariance matrix with the columns stacked in a single column vector and $\mathbf{M} = \overline{\mathbf{A}} \circ \mathbf{A}$, where $\circ$ denotes the Khatri-Rao product or column-wise Kronecker product and $\overline{\cdot}$ denotes conjugation. Using covariance matched weighting

($\mathbf{W} = \overline{\mathbf{R}}^{-1/2} \otimes \mathbf{R}^{-1/2}$, where $\otimes$ denotes the Kronecker product), the weighted LS estimate is asymptotically equivalent to the maximum likelihood estimate [9]. It is straightforward to extend this vectorized formulation to include multiple snapshots over time and frequency to improve the imaging result [8]. Although we will use this extension in Sec. 4, we will present the image reconstruction based on this single snapshot model for clarity of presentation.

A closed form solution can be found by solving for $\boldsymbol{\sigma}_{\mathrm{n}}$ as function of $\boldsymbol{\sigma}$ and substituting the solution back into the cost function. The imaging problem can then be formulated as [8]

$$\widehat{\boldsymbol{\sigma}} = \underset{\boldsymbol{\sigma}}{\operatorname{argmin}} \left\| \widetilde{\mathbf{W}} \left(\widehat{\mathbf{r}} - \mathbf{M}\boldsymbol{\sigma} \right) \right\|_{\mathrm{F}}^{2}, \tag{3}$$

where

$$\widetilde{\mathbf{W}} = \mathbf{W} - \mathbf{W}\mathbf{M}_{\mathrm{n}} \left(\mathbf{M}_{\mathrm{n}}^{H} \mathbf{W}^{H} \mathbf{W} \mathbf{M}_{\mathrm{n}} \right)^{-1} \mathbf{M}_{\mathrm{n}}^{H} \mathbf{W}^{H} \mathbf{W}. \tag{4}$$

This modified weighting matrix can be interpreted as a filter to remove the noise source signature from the data. If there are no noise signals, (2) reduces to

$$\widehat{\boldsymbol{\sigma}} = \underset{\boldsymbol{\sigma}}{\operatorname{argmin}} \left\| \mathbf{W} \left(\widehat{\mathbf{r}} - \mathbf{M}\boldsymbol{\sigma} \right) \right\|_{\mathrm{F}}^{2}. \tag{5}$$

Since the only difference between the general and the noise free case is in the contents of the weighting matrix, we will use (5) in the remainder of the paper.

The standard solution to the image reconstruction problem formulated in (5) is

$$\widehat{\boldsymbol{\sigma}} = \left(\mathbf{W}\mathbf{M} \right)^{\dagger} \mathbf{W}\widehat{\mathbf{r}} = \mathbf{M}_{\mathrm{d}}^{-1} \boldsymbol{\sigma}_{\mathrm{d}}, \tag{6}$$

where † denotes the pseudo-inverse. We also introduced the dirty image $\boldsymbol{\sigma}_{\mathrm{d}} = \mathbf{M}^{H}\mathbf{W}^{H}\mathbf{W}\widehat{\mathbf{r}}$ and the deconvolution matrix $\mathbf{M}_{\mathrm{d}} = \mathbf{M}^{H}\mathbf{W}^{H}\mathbf{W}\mathbf{M}$. The dirty image can be computed from the data without an inversion and shows the true image convolved with the spatial response of the array. The multiplication with the inverse of the deconvolution matrix removes the instrumental response and should thus result in the true image. The condition number of the deconvolution matrix strongly depends on the chosen image grid. If the image resolution is chosen too high, the problem becomes ill-posed and inversion is not possible without introducing some form of regularization.

3. PROPOSED METHOD

If the dimensionality of $\boldsymbol{\sigma}$ is chosen too large by the user such that the deconvolution matrix cannot be properly inverted, this implies that the amount of information contained in the Q pixels, which are assumed to be mutually independent, is larger than the amount of information available in the data and that some form of regularization is required to constrain the problem. This will reparameterize the problem to a parameter vector $\boldsymbol{\theta}$ with length smaller than Q.

The KLT offers a way to find a data dependent set of base vectors. It uses an eigenvalue decomposition of the parameter vector covariance matrix, $\mathbf{C}_{\boldsymbol{\sigma}}$. Since the celestial source signals are spatially uncorrelated, we would therefore like to assume that the pixel values are uncorrelated, i.e., that $\mathbf{C}_{\boldsymbol{\sigma}}$ is diagonal. In that case, however, the eigenvalue decomposition will provide the user specified pixels as base functions. This works if the sky is mostly empty, a key assumption of the commonly used CLEAN method [10] for image reconstruction in radio astronomy. Unfortunately, some datasets contain more structure than only point sources as illustrated in the next section. These images are hard to handle with the CLEAN technique. The sources found using the CLEAN technique are commonly convolved with a smooth, typically Gaussian, function to restore the image resolution provided by the instrument thereby avoiding overinterpretation of the data. This recognizes the fact that neighboring pixel values have a higher covariance than well-separated pixel values due to the limited resolution provided by the instrument.

This suggests that $\mathbf{C}_{\boldsymbol{\sigma}}$ could be described by the true image convolved with a Gaussian function. This approach has several disadvantages. First, the true image is unknown, so this would lead to an iterative and computationally expensive approach. Second, the user would still need to tune the image resolution, not by specifying the image grid but by specifying the width of the Gaussian deconvolution function. Finally, the resolution provided by a phased array measurement may vary with direction.

We therefore propose a different approach based on the observation that the dirty image $\boldsymbol{\sigma}_{\mathrm{d}}$ and the true image $\boldsymbol{\sigma}$ describe the same physical space. This implies that if the true image can be linearly mapped on a lower dimensional space, the dirty image should be linearly projectable on the same space. This is an important observation, since the dirty image can be derived from the data without inversion and therefore the covariance of the dirty image can be calculated from the covariance of the data. We thus propose to use the base functions $\mathbf{U}_{\boldsymbol{\theta}}$ obtained as the set of significant eigenvectors, i.e. eigenvectors associated with the signal subspace, of the dirty image covariance matrix $\mathbf{C}_{\boldsymbol{\sigma}_{\mathrm{d}}}$, i.e., from

$$\mathbf{C}_{\boldsymbol{\sigma}_{\mathrm{d}}} = \mathbf{U}\boldsymbol{\Lambda}\mathbf{U}^{H} \approx \mathbf{U}_{\boldsymbol{\theta}}\boldsymbol{\Lambda}_{\boldsymbol{\theta}}\mathbf{U}_{\boldsymbol{\theta}}^{H}. \tag{7}$$

For Gaussian signals, the data covariance is known to be $\left(\overline{\mathbf{R}} \otimes \mathbf{R} \right) / N$, where N is the number of samples over which the data are integrated. The covariance of the dirty image vector can then be described as

$$\mathbf{C}_{\boldsymbol{\sigma}_{\mathrm{d}}} = \frac{1}{N} \mathbf{M}^{H}\mathbf{W}^{H}\mathbf{W} \left(\overline{\mathbf{R}} \otimes \mathbf{R} \right) \mathbf{W}^{H}\mathbf{W}\mathbf{M}. \tag{8}$$

If we substitute the data model given by (1) and simplify the result, we find that

$$\mathbf{C}_{\boldsymbol{\sigma}_{\mathrm{d}}} = \mathbf{M}_{\mathrm{d}}, \tag{9}$$

i.e., that the covariance of the dirty image vector is simply the deconvolution matrix. This is an intuitive result since the deconvolution matrix describes how the image values are related

to each other via the directional response of the receiving array. This demonstrates that base functions obtained from the KLT only depend on the observed signal and the directional response of the instrument, i.e., they only depend on intrinsic physical properties of the measurement setup and not on assumptions made by the user.

With these base functions, the solution follows from

$$\widetilde{\boldsymbol{\sigma}} = \mathbf{U}_{\boldsymbol{\theta}} \boldsymbol{\Lambda}_{\boldsymbol{\theta}}^{-1} \mathbf{U}_{\boldsymbol{\theta}}^{H} \boldsymbol{\sigma}_{\mathrm{d}}, \tag{10}$$

which is the pseudo-inverse commonly used for noisy cases. The inversion is thus reduced to inverting a diagonal matrix. The condition number of $\boldsymbol{\Lambda}_{\boldsymbol{\theta}}$ depends on the number of base functions selected.

Note that we do not compute $\boldsymbol{\theta}$ explicitly. Using $\boldsymbol{\theta} = \mathbf{U}_{\boldsymbol{\theta}}^{H} \boldsymbol{\sigma}$, it is still possible to formulate the maximum a-posteriori (MAP) estimator as [11]

$$\widehat{\boldsymbol{\sigma}} = \underset{\boldsymbol{\sigma}}{\operatorname{argmin}} \left\| \mathbf{W} \left(\widehat{\mathbf{r}} - \mathbf{M}\boldsymbol{\sigma} \right) \right\|_{\mathrm{F}}^{2} + \left\| \boldsymbol{\Lambda}_{\boldsymbol{\theta}}^{-1/2} \mathbf{U}_{\boldsymbol{\theta}}^{H} \boldsymbol{\sigma} \right\|_{\mathrm{F}}^{2}, \tag{11}$$

which can be optimized by trying different dimensionalities for $\mathbf{U}_{\boldsymbol{\theta}}$. The MAP formulation thus provides a clear criterion to limit the number of base vectors used for image reconstruction, but this is a computationally intensive process. In the demonstration in the next section, we will impose a restriction on the condition number of $\boldsymbol{\Lambda}_{\boldsymbol{\theta}}$ instead to ensure proper inversion given the SNR of the data.

4. EXPERIMENTAL RESULTS

We demonstrate our proposed method using actual data from the low frequency array (LOFAR). LOFAR is a phased array radio telescope, built in the Netherlands, covering the 10 – 250 MHz frequency range [7]. It consists of 48 stations with two types of antennas. For our demonstration we used the low band antennas, operating between 10 and 90 MHz, of a single station. The antennas were arranged in a randomized configuration with 82 m diameter.

The data were captured on November 6, 2008 between 10:22:21 and 10:26:45 UTC. The data consisted of 25 10-s observations in 25 distinct 156 kHz frequency channels between 45.156 and 67.188 MHz. The channels were selected to provide even coverage of the given frequency range taking into account the locally present radio frequency interference.

For comparison, the first image was made using LS image reconstruction without regularization. The resolution of a radio telescope with a completely filled untapered aperture is roughly λ/D radians [12], where λ is the observed wavelength and D is the diameter of the aperture. To show the limits of LS image reconstruction, we set the spacing in the image grid to $0.8\lambda/D$ taking $\lambda = 4.47$ m, the wavelength at the highest frequency. The result is shown in Fig. 1. The image is sampled on a regular grid by projecting the hemisphere on the horizon plane of the aperture array, which exactly compensates for beam elongation with increasing bore sight angle.

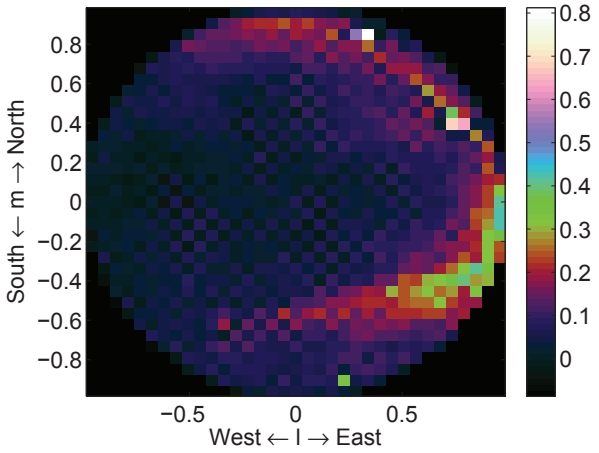

Fig. 1. Hemispheric image obtained from unregularized LS image reconstruction. The resolution is $0.8\lambda/D$ where λ is the wavelength at the highest frequency.

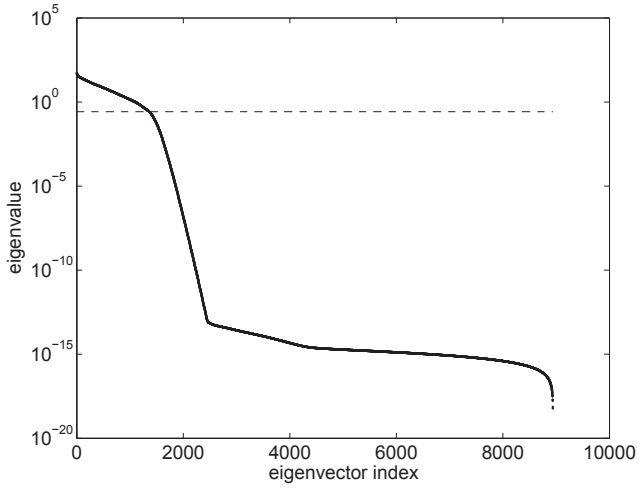

Fig. 2. Eigenvalues of the dirty image covariance matrix.

The image looks coarse, because the size of the pixels is close to the resolution of the telescope. Even with this resolution, the image reconstruction process already produces a checkerboard pattern over the image, indicating that we are pushing the limits of the inversion, i.e., we can hardly extract more independent information from the data.

To get a more natural looking image and to demonstrate that the proposed method allows to define the grid spacing without worrying about the tractability of the inversion problem, we made the image grid spacing three times as small increasing the number of pixels in the image from 989 to 8937. Figure 2 shows the eigenvalues of the dirty image covariance

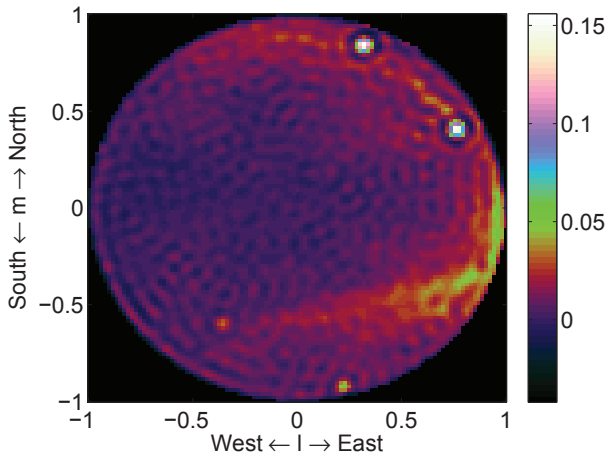

Fig. 3. The same hemispheric image as shown in Fig. 1 obtained using the KLT. The specified image resolution is three times higher than in the LS optimized image.

matrix. The eigenvalues are gradually decreasing up to a certain cut-off where they decrease sharply to the limits of numerical accuracy, signifying the transition from the signal to the noise subspace. Picking a threshold close to this cut-off, we defined a threshold at $\lambda_{\max}/200$ leaving 1361 out of 8937 image components.

Figure 3 shows the image produced using the KLT. The Sun, visible near the southern horizon and Virgo A, the point source at the end of the diffuse emission on the southern hemisphere, are clearly visible in both images, but the image made using the KLT would provoke far less debate on whether these sources were real or imaging artefacts. The dark rings around the two bright sources near the northeastern horizon, Cassiopeia A and Cygnus A, result from the tendency of LS techniques to smooth sharp features. In radio astronomy, strong sources often get special treatment and some people have proposed to use the l_1-norm instead in image reconstruction problems [1]. Since the horizon forms a sharp edge, the tendency of the LS optimization to smooth sharp edges may also explain the circular ripples that appear to come from the horizon. This may improve by adding a realistic beam model, since the lower sensitivity of the receiving elements towards the horizon forms a natural taper.

5. CONCLUSIONS

Many image reconstruction problems are ill-posed and therefore require some form of regularization. We proposed a data driven model based LS image reconstruction technique using base functions obtained from the KLT to describe the image. These base functions are derived from the covariance matrix of the pixels in the dirty image. This is the true image convolved with the instrumental response. The chosen base functions are based on intrinsic physical properties of the measurement process and do not introduce any subjective regularization criterion that may bias the solution. We successfully demonstrated the proposed method on actual radio interferometric data from the LOFAR instrument.

6. REFERENCES

[1] Ronny Levanda and Amir Leshem, "Synthetic Aperture Radio Telescopes," *IEEE Signal Processing Magazine*, vol. 27, no. 1, pp. 14–29, Jan. 2010.

[2] Jeffrey A. Fessler, "Model-Based Image Reconstruction for MRI," *IEEE Signal Processing Magazine*, vol. 27, no. 4, pp. 81–89, July 2010.

[3] Paul Maarten Zwartjes, *Fourier reconstruction with sparse inversion*, Ph.D. thesis, Delft University of Technology, Delft, The Netherlands, Dec. 2005.

[4] Charles V. Jakowatz et al., *Spotlight-mode synthetic aperture radar: a signal processing approach*, Kluser Academic Publishers, Dordrecht, The Netherlands, 1996.

[5] Stefan J. Wijnholds and Alle-Jan van der Veen, "Fundamental Imaging Limits of Radio Telescope Arrays," *IEEE Journal of Selected Topics in Signal Processing*, vol. 2, no. 5, pp. 613–623, Oct. 2008.

[6] Panagiotis Lampropoulos, *The LOFAR Epoch of Reionization experiment data model: Simulations, calibration and inversion*, Ph.D. thesis, University of Groningen, Groningen, The Netherlands, Sept. 2010.

[7] M. de Vos, A.W. Gunst, and R. Nijboer, "The LOFAR Telescope: System Architecture and Signal Processing," *Proceedings of the IEEE*, vol. 97, no. 8, pp. 1431–1437, Aug. 2009.

[8] Stefan J. Wijnholds, *Fish-Eye Observing with Phased Array Radio Telescopes*, Ph.D. thesis, Delft Unisversity of Technology, Delft, The Netherlands, Mar. 2010.

[9] B. Ottersten, P. Stoica, and R. Roy, "Covariance Matching Estimation Techniques for Array Signal Processing Applications," *Digital Signal Processing, A Review Journal*, vol. 8, pp. 185–210, July 1998.

[10] J. A. Högbom, "Aperture Synthesis with a Non-regular Distribution of Interferometer Baselines," *Astronomy & Astrophysics Supplement*, pp. 417–426, 1974.

[11] S. M. Kay, *Fundamentals of Statistical Signal Processing: Estimation Theory*, Prentice Hall, Upper Saddle River (New Jersey), USA, 1993.

[12] John D. Kraus, *Radio Astronomy*, Cygnus-Quasar Books, 2nd edition, 1986.